Proceedings of the XVIII ECSMGE 2024
GEOTECHNICAL ENGINEERING CHALLENGES
TO MEET CURRENT AND EMERGING NEEDS OF SOCIETY

ISBN 978-1-032-54816-6
DOI 10.1201/9781003431749-72

ECSMGE 24
XVIII EUROPEAN CONFERENCE ON SOIL MECHANICS AND GEOTECHNICAL ENGINEERING

Undrained triaxial test stress path shape as an indicator of sample quality

Forme du chemin de contrainte d'essai triaxial non drainé comme indicateur de la qualité de l'échantillon

V. Gjelsvik*, K. Kahrs
Norwegian Geotechnical Institute (NGI), Trondheim, Norway

**vidar.gjelsvik@ngi.no*

ABSTRACT: When determining soil strength parameters from laboratory tests for use in geotechnical safety evaluations, knowing the quality of the test sample is important. The quality of a triaxial test sample is commonly assessed by evaluating Δe (the change in void ratio during consolidation to the initial in situ stress)/e_0 (the initial void ratio). However, the type of behaviour of a sample during advanced testing can also provide information about the sample quality. We have analysed the stress paths of 89 active and passive anisotropically consolidated undrained triaxial tests on high quality block samples of clay with regard to shape, average dilatancy, and strain at failure and visualized the results in plots of the normalized shear stress against the overconsolidation ratio. From those plots, typical regions where points with a certain stress path shape, average dilatancy, or strain at failure can be identified as well as outliers. Our analysis indicates that outliers typically are points with a lower sample quality.

RÉSUMÉ: La qualité d'un échantillon d'argile est très importante afin de bien évaluer les paramètres de résistance du sol à l'aide d'essais en laboratoire. La qualité d'un échantillon d'essai triaxial est généralement évaluée en analysant le changement de l'indice des vides (Δe) pendant la consolidation de l'échantillon par rapport à l'indice des vides initial (e_0). Cependant, le comportement du sol pendant l'essai triaxial peut également en dire long sur la qualité de l'échantillon. Dans ce papier nous avons analysé les chemins de contrainte de 89 essais triaxiaux actifs et passifs non drainés et consolidés anisotropiquement sur des échantillons de bloc d'argile de haute qualité. L'analyse compare les différents chemins de contrainte par rapport à leur forme, la dilatance moyenne de l'échantillon et la déformation à la rupture. Les résultats sont comparés et visualisés en utilisant la contrainte de cisaillement normalisée en fonction du degré de sur-consolidation. La méthode présentée dans ce papier permet d'identifier des valeurs aberrantes en comparant avec la forme des cheminements de contrainte, la dilatance moyenne ou la déformation à la rupture. Notre analyse indique que les valeurs aberrantes sont généralement des points avec une qualité d'échantillon inférieure.

Keywords: Triaxial test stress path; overconsolidation ratio; dilatancy; sample quality.

1 INTRODUCTION

When determining soil strength parameters from laboratory tests for use in geotechnical safety evaluations, knowing the quality of the sample is important. There are well-established methods for quantifying sample quality for advanced tests such as triaxial and oedometer tests (Lunne et al., 1997; Karlsrud and Hernandez-Martinez, 2013; Berre et al., 2022). However, the behaviour of a sample during advanced testing also provides information about sample quality (e.g. Paniagua et al., 2017). Strength parameters from triaxial tests are usually determined graphically from a stress path plot. In this project, we have analysed the stress paths of 89 anisotropically consolidated undrained active (CAUc) and passive triaxial (CAUe) tests performed on high quality block samples of clay with regard to shape, average dilatancy before failure, and strain at failure. This paper demonstrates typical signs of good sample quality and gives examples of the expected behaviour for clays with overconsolidation ratios (OCRs) between 1 and 6.

2 ASSESSMENT OF SAMPLE QUALITY

The quality of a triaxial test sample is commonly assessed according to the classification given in ISO standard 19901-8:2014. The classification is based on the ratio between the change in void ratio during consolidation of the sample to in situ stresses (Δe) and the initial void ratio (e_0) and was originally proposed by Lunne et al. (1997). The extended classification for OCRs between 1 and 6 proposed by the Norwegian Geotechnical Society (NGF, 2013) is presented in Table 1.

Table 1. Evaluation of sample quality (NGF, 2013).

OCR	$\Delta e/e_0$			
1 to 2	<0.04	0.04-0.07	0.07-0.14	>0.14
2 to 4	<0.03	0.03-0.05	0.05-0.10	>0.10
4 to 6	<0.02	0.02-0.035	0.035-0.07	>0.07
Quality	1	2	3	4

1 very good to excellent, 2 fair to good, 3 poor, 4 very poor

Earlier studies have shown that piston samples with excellent quality according to the $\Delta e/e_0$-criterion still could have considerable disturbance compared to block samples (Paniagua et al., 2017; L'Heureux et al., 2018), measured by the undrained shear resistance. Therefore, the authors believe that data presented in this article could be useful in the overall assessment of clay sample disturbance.

3 DATA

We have used data from anisotropically consolidated undrained active (CAUc) and passive (CAUe) triaxial tests performed on high quality (class 1 or class 2) Ø250 mm block samples of clay from NGI's GEODIP high quality database (NGI, 2018). All triaxial tests in the database are consolidated to the assumed in situ stress state before shearing. An overview of the test sites with the number of CAUc and CAUe tests used from each site is given in (NGI, 2018). Table 2 shows the range of basic parameters in the database.

Table 2 Range of basic properties

Parameter	**Range**
w (%)	25 – 55
γ_t (kN/m³)	17 – 20
Clay content (%)	20 – 60
I_p (%)	5 – 30
S_t	2 – 225
OCR	1.1 – 6.2

The triaxial test data is visualized below by means of a stress -strain plot where $t = \frac{\sigma_a - \sigma_r}{2}$ (Figure 1) and a MIT stress path plot, where $s' = \frac{\sigma'_a + \sigma_r'}{2}$ (Figure 2). The stresses are normalized by the assumed in situ effective vertical stress.

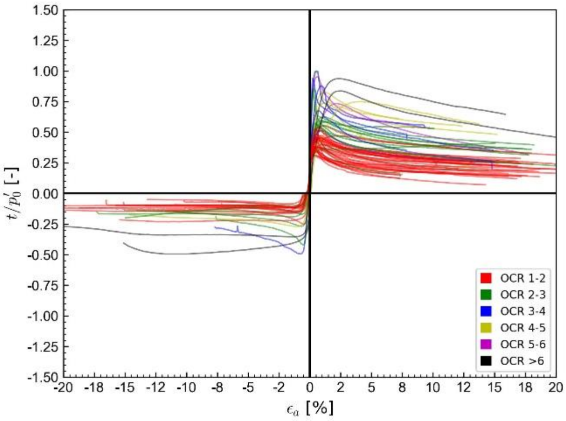

Figure 1. A normalized stress-strain plot visualizing the results from all active and passive triaxial tests.

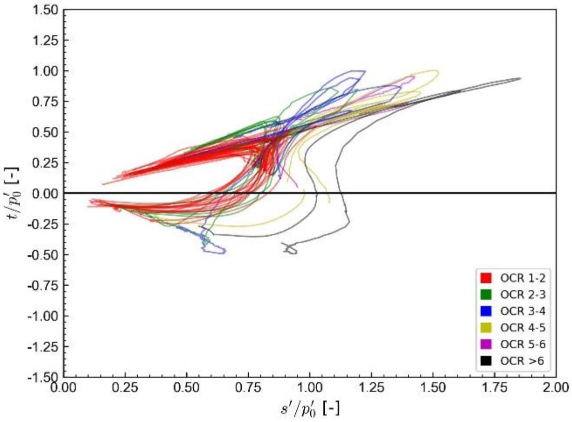

Figure 2. A normalized NGI/MIT stress path plot visualizing the results from all active and passive triaxial tests.

4 METHOD

4.1 Stress path shape

We have plotted the stress path of each active and passive triaxial test in a normalized MIT plot. The stress paths can be seen to group into four distinct types of shape according to the sample's dilative and contractive behaviour in shear just before and after failure: (1) a "contraction only" shape with a rounded turning point, (2) a "slight dilation, then contraction" shape with a sharp turning point either to the left or to the right of the zero dilatancy line (typically CAUc) or a loop to the left of the zero dilatancy line (typically CAUe), (3) a "dilation, then contraction" type with a looping turning point (pigs tail) to the right of the zero dilatancy line, and (4) a "dilation only" shape without a turning point. Our data does not contain any samples with stress path type 4.

Typical examples of shape types 1, 2, and 3 are given in Table 3. For each example, we have shown the stress path corresponding to zero dilatancy, which in an MIT plot is a straight line with gradient 3.

Table 3. Typical examples of stress path shape types 1-3.

Type	CAUC	CAUE
1	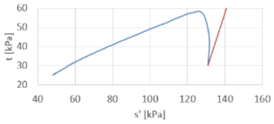	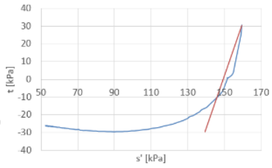
2	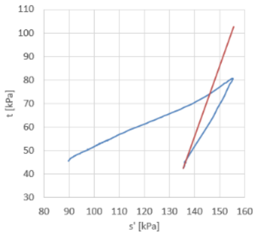	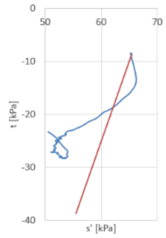
3	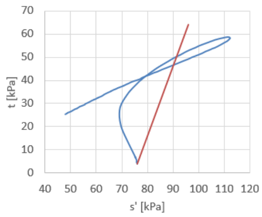	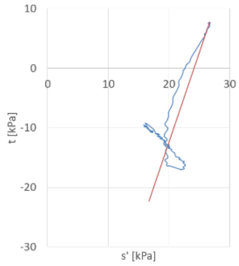

4.2 Average dilatancy

The average dilatancy is computed as the dilatancy between the initial stress state and the stress state at failure:

$$\overline{D} = \frac{\Delta\sigma'_m}{\Delta\sigma_d} = \frac{\sigma'_{m,f} - \sigma'_{m,0}}{\sigma_{d,f} - \sigma_{d,0}} \qquad (1)$$

where σ_d (kPa) is the deviatoric stress and σ'_m (kPa) is the effective octahedral stress. For tests where failure occurs at an axial strain greater than 10%, the stress state at 10% axial strain is used. The average gradient from initial state to failure in the MIT-plot is:

$$\frac{\Delta t}{\Delta s'} = \frac{3}{1+6\overline{D}} \qquad (2)$$

4.3 Axial strain at failure, maximum shear stress, and overconsolidation ratio

The axial strain at failure, the shear strength, and the overconsolidation ratio at the depth of the triaxial test sample are provided in the GEODIP database and used directly. For tests where failure occurs at an axial strain greater than 10%, an axial strain of 10% and a shear strength equal to the shear stress at 10% axial strain are used.

5 RESULTS

The results are shown in plots of the normalized shear strength c_u/p'_0 against the OCR where each data point corresponds to one of the 89 triaxial tests. The data point colours correspond to different stress path types (Figure 3), different ranges of average dilatancy (Figure 4), and different ranges of axial strain at failure (Figure 5).

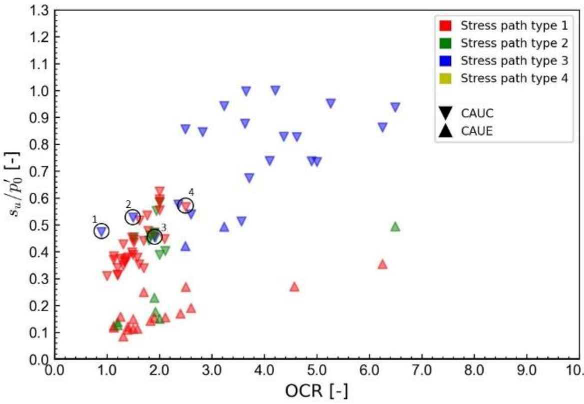

Figure 3. Normalized shear strength plotted against OCR. The data point colours correspond to stress path types 1-4.

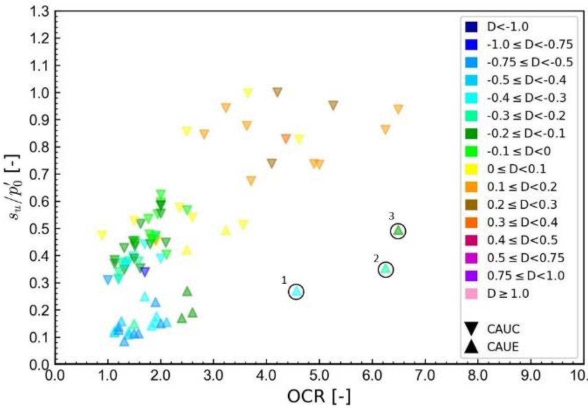

Figure 4. Normalized shear strength plotted against OCR. The data point colours correspond to different ranges of average dilatancy, $\overline{D}$.

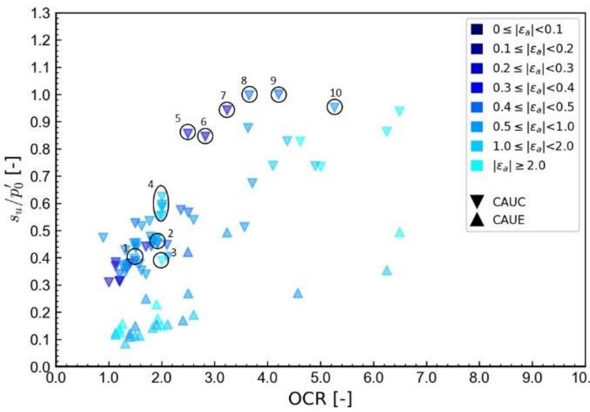

Figure 5. Normalized shear strength plotted against OCR. The data point colours correspond to different ranges of axial strain at failure.

6 DISCUSSION

For active triaxial tests, we see that stress path type 1 generally occurs for OCRs between 1 and 2, type 2 for OCRs around 2, and type 3 for OCRs larger than 2.5. For passive triaxial tests, there is no such pattern. We have marked four outliers in Figure 3. Outliers 1-3 are stress path type 3 samples that are very close to having stress path type 2 (very small loop). Outlier 4 is a stress path type 1 sample that dilates up to a shear stress of almost 50% of the maximum shear stress, so this sample is close to having stress path type 2.

In Figure 4, we see that for active triaxial tests there is a general trend of the average dilatancy increasing from large negative values (contraction) to large positive values (dilation) with increasing OCR and normalized shear strength. The results clearly demonstrate the mechanism behind the well-known stress history dependence, described in the SHANSEP procedure (Ladd and Foott, 1974). This OCR dependency can also be seen for passive triaxial tests, but only for OCR values less than 3.2. There are, however, few passive triaxial test samples with OCRs larger than 3.2. All three of those samples (marked 1, 2, and 3 in Figure 4) are of quality 2. More data is needed to conclude on whether those samples are outliers or whether there is more scatter in the CAUe data than in the CAUc data. The gradient, $\frac{\Delta t}{\Delta s'}$ ranges from about $-\frac{6}{7}$ for NC-clays to $+\frac{1}{1}$ for OC-clays, noting that also the initial stress state ranges from K_0' = 0,55 – 1,0 for NC- to OC-clays respectively.

In Figure 5, we see that for active triaxial tests there is a general trend of the axial strain at failure increasing with increasing OCR and normalized shear strength. For passive triaxial tests, there is a lot more scatter in the data, and no clear trend can be seen. In particular, there are many CAUe samples with low OCRs that fail at a high axial strain. We have marked ten outliers among the CAUc data points. Outliers 1, 2, and most of the test samples marked as outlier 4, which exhibit a higher axial strain at failure than what would be expected from the general trend in the data, are from sites Onsøy and Bothkennar. Those sites have high plasticity (I_p above 30%) relative to the other sites. Outliers 5-10, which exhibit a lower axial strain than expected, are from site Emmerstad. The clay from this site is probably cemented. Outlier 3 has a stress-strain curve that is known to be typical of samples that have been disturbed.

7 CONCLUSIONS

In this paper, we have provided three plots that visualize a high quality undrained triaxial test sample's typical behaviour in undrained shear with regard to the shape of the stress path, the average dilatancy, and the axial strain at failure. For active tests, regions where samples with a given overconsolidation ratio typically will plot can be identified. Outliers are typically samples of a lower quality or with material characteristics that differ from those of most of the other samples. To improve the plots' usefulness as a tool for visually assessing sample quality, it may be necessary to create separate plots for clays with different material characteristics. For passive tests, there is more scatter in the data, and more data with overconsolidation ratios larger than 3 is needed to conclude on whether similar regions can be identified here.

ACKNOWLEDGEMENTS

The project presented in this article was funded in part by the Norwegian Research Council through the Strategic Research Project SP8-GEODIP at NGI.

REFERENCES

Berre, T., Lunne, T., & L'Heureux, J. S. (2022). Quantification of sample disturbance for soft, lightly overconsolidated, sensitive clay samples. *Canadian Geotechnical Journal*, *59*(2), 300-303

Karlsrud, K. and Hernandez-Martinez,F. G. (2013). Strength and deformation properties of Norwegian clays from laboratory tests on high-quality block samples. *Can. Geotech. J.*, 50(12): 1273-1293. http://doi.org/10.1139/cgj-2013-0298

Lunne, T., Berre, T. and Strandvik, S. (1997). Sample disturbance effects in soft low plastic Norwegian clay. In: *Recent Developments in Soil and Pavement Mechanics*, Almeida (ed.), Balkema, Rotterdam, Netherlands, pp. 81-102.

NGF (2013). Melding 11 Veiledning for prøvetaking (Guidelines for sampling), Norsk Geoteknisk Forening. Oslo, Norway (in Norwegian).

NGI (2018). SP8 – Soil Parameters in Geotechnical Design (GEODIP). GEODIP's high-quality database: Clay, Norwegian Geotechnical Institute, Oslo, Norway, Rep. 20150030-02-R rev. 2.

Paniagua, P., L'Heureux, J.-S., Carroll, R., Kåsin, K. and Sjursen, M. (2017). Evaluation of sample disturbance of three Norwegian clays. In: *Proceedings of the 19th International Conference on Soil Mechanics and Geotechnical Engineering*, Seoul, South Korea, pp. 481-484.